Research paper

Understanding the adsorption mechanism of chitosan onto poly(lactide-co-glycolide) particles

Chunqiang Guo [a], Richard A. Gemeinhart [a,b,*]

[a] Department of Biopharmaceutical Sciences, University of Illinois, Chicago, IL, USA
[b] Department of Bioengineering, University of Illinois, Chicago, IL, USA

ARTICLE INFO

ABSTRACT

Polyelectrolyte-coated nanoparticles or microparticles interact with bioactive molecules (peptides, proteins or nucleic acids) and have been proposed as delivery systems for these molecules. However, the mechanism of adsorption of polyelectrolyte onto particles remains unsolved. In this study, cationic poly(lactide-co-glycolide) (PLGA) nanoparticles were fabricated by adsorption of various concentrations of a biodegradable polysaccharide, chitosan (0–2.4 g/L), using oil-in-water emulsion and solvent evaporation techniques. The particle diameter, zeta-potential, and chitosan adsorption of chitosan-coated PLGA nanoparticles confirmed the increase of polyelectrolyte adsorption. Five adsorption isotherm models (Langmuir, Freundlich, Halsey, Henderson, and Smith) were applied to the experimental data in order to better understand the mechanism of adsorption. Both particle diameter and chitosan adsorption increased with chitosan concentration during adsorption. A good correlation was obtained between PLGA-chitosan nanoparticle size and adsorbed chitosan on the surface, suggesting that the increased particle size was primarily due to the increased chitosan adsorption. The zeta-potential of chitosan-coated PLGA nanoparticles was positive and increased with chitosan adsorbed until a maximum value (+55 mV) was reached at approximately 0.4–0.6 g/L; PLGA nanoparticles had a negative zeta-potential (−20 mV) prior to chitosan adsorption. Chitosan adsorption on PLGA nanoparticles followed a multilayer adsorption behavior, although the Langmuir monolayer equation held at low concentrations of chitosan. The underlying reasons for adsorption of chitosan on PLGA nanoparticles were thought to be the cationic nature of chitosan, high surface energy and microporous non-uniform surface of PLGA nanoparticles.

© 2008 Elsevier B.V. All rights reserved.

1. Introduction

Poly(lactide-co-glycolide) microparticles (MPs) and nanoparticles (PLGA NPs) have been extensively studied as drug carriers based upon the properties of degradability and biocompatibility [1,2]. Small molecule and biomacromolecular therapeutics, e.g. peptides, proteins, or nucleic acids, can be loaded into PLGA particles to achieve a controlled release and protection from degradation. However, the lack of functional groups on the surface of PLGA NPs for covalent modification has limited the potential for surface tethering bioactive molecules including DNA, ligands [3] or vaccines [4]. Thus, various attempts for physical surface modification of PLGA NPs have been made by coating PLGA with surfactants or polymers. As such, cationic surface modification based upon the electrostatic interaction with the negatively charged surface of PLGA has been suggested as a potential method to modify the surface of PLGA NPs [5].

Although negatively charged and neutral particles may be more advantageous for systemic administration in the blood [6], cationic particles are useful drug carriers especially for DNA, proteins and peptide [5,7]. Since the cell membrane is negatively charged, cationic particles can easily interact with the cell membrane and promote subsequent bioactivity. In particular, cationic particles have been actively investigated for gene delivery based on electrostatic interaction between cationic particles and negatively charged DNA. Cetyl trimethyl ammonium bromide (CTAB), as a cationic surfactant, has been applied to coat PLGA cationic particles for efficient DNA vaccine delivery [8,9]. Cationic polymers, including polyethyleneimine (PEI) [10–12], polylysine [13], chitosan [14,15], and gelatin [16], have also been reported as coating materials for biodegradable PLGA or poly (D,L-lactic acid) particles [17] as gene carriers. Cationic surface modification of nanoparticles can be obtained either during the formation of PLGA particles or by incubating polyelectrolytes with preformed

* Corresponding author. Associate Professor of Pharmaceutics and Bioengineering, Department of Biopharmaceutical Sciences, College of Pharmacy, University of Illinois, 833 South Wood Street (MC 865), Chicago, IL 60612-7231, USA. Tel.: +1 312 996 2253; fax: +1 312 996 2784.
E-mail address: rag@uic.edu (R.A. Gemeinhart).

PLGA particles [16], using emulsion-solvent evaporation or spray-drying techniques.

PLGA particle coating with surfactants or polymers is fundamentally an interfacial phenomenon, regardless of whether adsorption is physical or chemical in nature. As such, polyelectrolyte adsorption to any surface can be affected by charge density, particle size, pH, ionic strength and temperature. In addition, adsorption phenomena can be studied in terms of thermodynamics or kinetics.

Chitosan-coated PLGA nanoparticles (chitosan-PLGA NPs) have been studied for mucosal gene delivery and were shown to facilitate gene delivery and protein expression *in vitro* and *in vivo* with increased efficiency [15]. However, the mechanism of chitosan adsorption onto PLGA NPs has not been clearly investigated despite recent results suggesting that chitosan can be adsorbed to PLGA NPs [18]. Adsorption of chitosan onto poly(D,L-lactic acid) was studied as potential DNA carriers, but little detail was given to the mechanism or extent of adsorption. The data poorly fit the Langmuir model, suggesting that the interactions were not simple surface adsorption phenomena [19].

In this study, chitosan-PLGA NPs were prepared by combining various concentrations of chitosan with PLGA NPs. In order to elucidate the mechanism of adsorption, chitosan-PLGA NPs were characterized by particle size, zeta-potential, mass of adsorbed chitosan, and six adsorption isotherm models were applied to the experimental data obtained. In addition, factors including pH and ionic strength which can affect the interaction of chitosan and PLGA NPs were investigated.

2. Materials and methods

All chemicals were reagent grade and purchased from Fisher Scientific, unless otherwise stated.

2.1. Preparation of chitosan-PLGA nanoparticles

Poly(D,L-lactide-co-glycolide) (PLGA; Resomer® RG 502H; Boehringer Ingelheim) was dissolved in 3 mL of dichloromethane. Chitosan (88 kDa, 53 cps; 85% deacetylation, Aldrich Chemical Co.) was dissolved at various concentrations (0–2.4 g/mL) in 0.25 N HCl, with the pH being adjusted to 5.0 with sodium hydroxide before use. Chitosan-PLGA NPs were prepared by a one-step oil-in-water emulsion, solvent evaporation method. In brief, 100 mg of PLGA in dichloromethane was added into a mixture of chitosan and poly(vinyl alcohol) (PVA; 30–70 kD, Sigma Chemical Co.) solution and emulsified by ultrasonication (Sonicator®, Misonix Inc, Farmingdale, NY) on ice for 120 s with 20% power output, pulse duty 0.25 s per cycle. PVA, a nonionic hydrophilic polymer, was included as a stabilizer for the dispersion with constant concentration of 0.5% w/v for all groups during sonication. The formed emulsion was then stirred on a magnetic stir plate at room temperature for 20 h to evaporate dichloromethane. Double distilled water was added to the suspension to reach a final chitosan-PLGA NPs concentration of 5 g/L.

2.2. Physicochemical characterization

Chitosan-PLGA NP hydrodynamic diameter was determined by quasi-elastic light scattering (QELS; Nicomp 370 Submicron Particle Size Analyzer, Santa Barbara, CA) using diluted dispersions in double distilled water. The scattering intensity fluctuation was measured at 90°, with a 10 min run time. The diameters were presented as volume-weighted data.

Prior to scanning electron microscopic examination, chitosan-PLGA NPs with or without wash were dried in a vacuum oven at −20 inches Hg directly after preparation. The washing of chitosan-PLGA NPs was repeated three times with distilled water and centrifuge. The dried samples were loaded onto a double adhesive carbon conductive tape (Ted Pella Inc., Redding, CA) or mica and coated with gold and palladium. Morphology was examined on a Hitachi S-3000N scanning electron microscope (Hitachi High Technologies America, Inc, Pleasanton, CA) or JEOL JSM-6320F microscope (JOEL Ltd., Tokyo, Japan), and digital micrographs were captured.

Surface charge of the nanoparticles was determined to be the voltage when static electrophoretic movement was observed by microscopy (Lazer Zee Meter®, Pen Kem, Inc., Bedford Hills, NY). Briefly, 1 mL of chitosan-PLGA suspension was diluted into approximately 25 mL of distilled deionized water before loading into the sample chamber. Zeta-potential of each sample was determined in distilled deionized water.

2.3. Chitosan adsorption

To determine the amount of chitosan adsorbed on the surface of chitosan-PLGA NPs, fluorescamine (Acros Organics; Morris Plains, NJ) was used due to its high sensitivity and specificity [20]. Fluorescence was generated by the reaction of fluorescamine with the primary amino groups of chitosan. Chitosan-PLGA NPs were centrifuged at 16,000g in a microcentrifuge (Eppendorf, Westbury, NY). A fluorescamine in DMSO solution (2.0 g/L) was added (100 μL) to the supernatant (20 μL) in a black 96-well fluorescent detection microplate. After reaction for 3 h while sheltered from light, fluorescence was measured at an excitation wavelength of 390 nm and emission wavelength of 515 nm using a SPECTRAmax® Gemini XS microplate spectrofluorometer (Molecular Devices, Sunnyvale, CA). A chitosan calibration curve was simultaneous run with each experiment. The mass of adsorbed chitosan on the PLGA NPs was calculated by subtracting the free chitosan in the supernatant from the initial feed, Eq. (1)

$$q = \frac{(C_i - C_e)V}{W} \tag{1}$$

where q is the amount of adsorbed chitosan on PLGA NPs, V is the volume of suspension (L), W is the mass of PLGA NPs, and C_i and C_e are the initial feed concentration of chitosan and the free chitosan concentration at equilibrium, respectively.

The volume of adsorbed layer of chitosan was calculated by subtracting the volume of an uncoated PLGA NP from that of a chitosan-PLGA NP with a spherical shape assumed [21]. The ratio of the mass of adsorbed chitosan per unit weight of PLGA versus the volume of adsorbed chitosan (defined as the density of adsorbed chitosan layer per unit weight of PLGA) was plotted against the initial chitosan concentration.

2.4. Adsorption isotherm model fitting

In order to understand the adsorption mechanism, the Langmuir [22], Eq. (2); BET [23], Eq. (3); Freundlich [24], Eq. (4); Halsey [25], Eq. (5); Henderson [26], Eq. (6); and Smith [27], Eq. (7) isotherm models were applied to the experimental adsorption data generated with a linearized form of the model [28–31] used when possible. In the equations, q is the mass of adsorbed chitosan per unit weight of PLGA particles and C_e is the equilibrium concentration of chitosan remaining in the solution. The other two parameters in each equation are constants related to either the adsorption capacity (q_m, k, and w_b) or the intensity of adsorption (b, n, and w_a).

$$\frac{C_e}{q} = \frac{1}{bq_m} + \frac{C_e}{q_m} \tag{2}$$

$$\frac{C_e}{q(1-C_e)} = \frac{1}{bq_m} + \frac{b-1}{bq_m}C_e \tag{3}$$

$$\log q = \log k + \frac{1}{n}\log C_e \tag{4}$$

$$\ln q = \frac{1}{n}\ln k - \frac{1}{n}\ln(-\ln C_e) \tag{5}$$

$$\ln[-\ln(1-C_e)] = \ln k + n\ln q \tag{6}$$

$$q = w_b - w_a \ln(1-C_e) \tag{7}$$

2.5. Data analysis

All data were expressed as means ± standard deviation and were compared using one-way ANOVA with subsequent Turkey's post-hoc test. Differences at a p-value less than 0.05 were considered to be statistically significant. All samples were examined in triplicate unless otherwise indicated, and all error bars are presented as standard deviations.
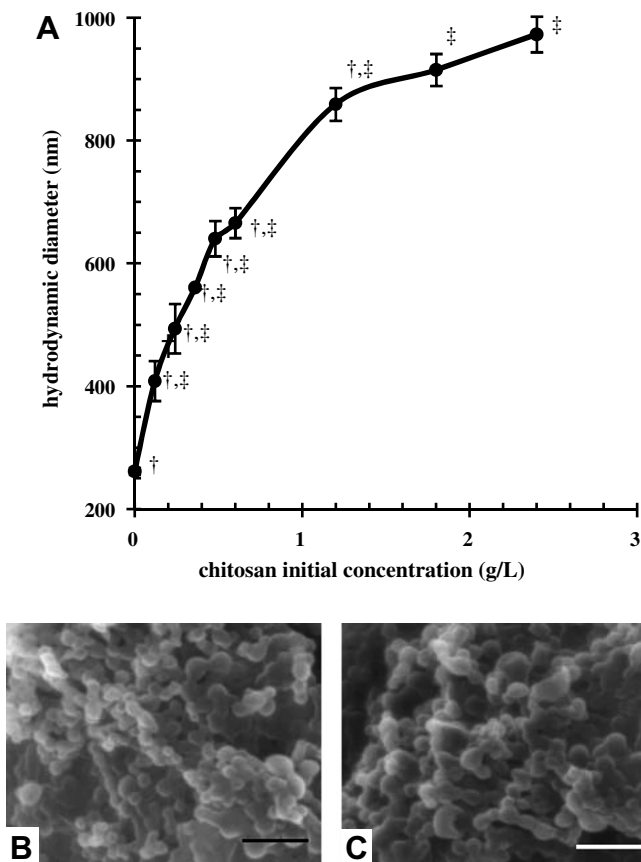
3. Results

3.1. Physicochemical characterization of nanoparticles

Chitosan-coated PLGA NPs were successfully and reproducibly manufactured. The hydrodynamic particle diameter was in the submicron range. The particle diameter distribution of chitosan-PLGA NPs was heterogeneous with two populations of particles regardless of the concentrations of chitosan. The average diameter (volume-weighted) of uncoated PLGA particles produced in PVA was 261.5 nm, which was smaller than the diameter of all the chitosan-coated NPs ($p < 0.05$). The mean diameter of chitosan-PLGA NPs increased steadily with chitosan feed concentrations ranging from 0.12 to 2.4 g/L (Fig. 1A). The largest particle diameter was 972.7 nm, which was obtained for PLGA NPs prepared at 2.4 g/L chitosan. Scanning electron microscopy revealed the spherical morphology of all particles (Fig. 1B and C). The particle diameters observed under scanning electron microscopy corroborate the diameters observed using quasi-elastic light scattering. The texture of the particle surface and shape was morphologically heterogeneous for both washed PLGA uncoated particles or washed chitosan-PLGA particles.

PLGA NPs produced in poly(vinyl alcohol) were electronegative, −20.3 mV, while all chitosan-coated PLGA NPs were electropositive ($p < 0.05$). The zeta-potential of chitosan-coated PLGA NPs increased with chitosan feed concentrations until a zeta-potential plateau was reached at approximately +55 mV when produced in a chitosan concentration of approximately 0.4–0.6 g/L (Fig. 2).

3.2. Chitosan adsorption

The amount of absorbed chitosan per gram of PLGA NPs increased with initial chitosan concentrations for the entire range (0–2.4 g/L) of chitosan concentrations examined (Fig. 3A). Unlike zeta-potential, there was no plateau of adsorption saturation for the chitosan concentrations tested. The highest mass of adsorbed chitosan was obtained at 2.4 g/L initial chitosan concentration with
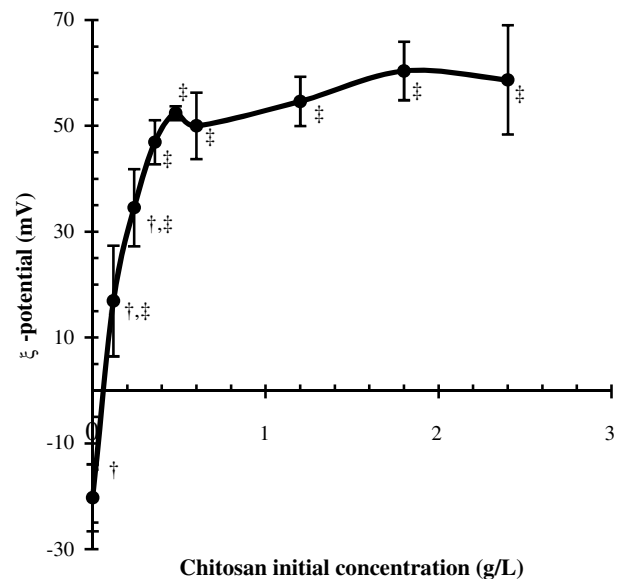

Fig. 1. Particle diameter and morphology of chitosan-PLGA particles made by the oil-in-water single emulsion-solvent evaporation method. (A) Particle diameter, as determined by quasi-elastic light scattering, of chitosan-PLGA NPs manufactured in increasing concentrations of chitosan which was combined with a set concentration of poly(vinyl alcohol). Values are presented as mean plus or minus standard deviation ($n = 3$) where ‡ represents a statistical difference ($p < 0.05$) compared to PLGA NPs made in 0 g/L chitosan and † represents statistical difference ($p < 0.05$) compared to PLGA NPs made in 2.4 g/L chitosan. (B) Representative scanning electron micrograph of uncoated PLGA NPs produced in poly(vinyl alcohol), i.e. without chitosan. (C) Representative scanning electron micrograph of chitosan-PLGA NPs made in 0.12 g/L chitosan. The scale bar in each micrograph is 1 μm.

Fig. 2. Effect of dispersed chitosan concentration on the zeta-potential of chitosan-PLGA microparticles prepared by the oil-in-water single emulsion solvent evaporation method. Values are presented as mean plus or minus standard deviation ($n = 3$) where ‡ represents a statistical difference ($p < 0.05$) compared to PLGA NPs made in 0 g/L chitosan and † represents statistical difference ($p < 0.05$) compared to PLGA NPs made in 2.4 g/L chitosan.
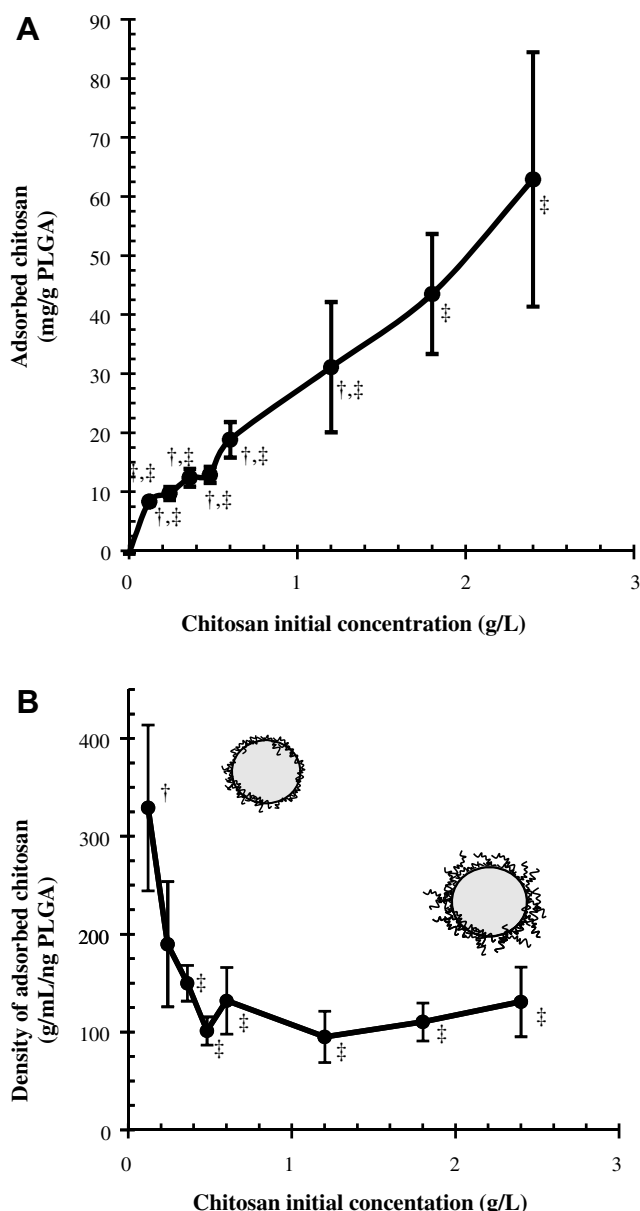
Fig. 3. Effect of dispersed chitosan concentration on the amount of chitosan absorbed onto PLGA NPs. The fluorescamine method was used to determine chitosan using Eq. (1). (A) Chitosan adsorbed to the surface of microparticles as a function of initial chitosan concentration. This data was replotted as Fig. 4 using each of the adsorption isotherm models. (B) Re-evaluation of the effect of chitosan absorption on the density of the chitosan layer. Values are presented as means ± standard deviation ($n = 3$) where ‡ represents a statistical difference ($p < 0.05$) compared to PLGA NPs made in 0 g/L in (A) and 0.12 g/L in (B) chitosan and † represents statistical difference ($p < 0.05$) compared to PLGA NPs made in 2.4 g/L chitosan.

62.9 mg per g of PLGA NPs ($p < 0.05$ compared to uncoated NPs). It should be noted that the amount of chitosan absorbed at higher (greater than about 1 g/L) initial chitosan concentrations resulted in increased variation as demonstrated by the standard deviation.

The chitosan density (mass of absorbed chitosan per volume of adsorbed chitosan layer) on the PLGA NPs was plotted against the initial chitosan concentrations (Fig. 3B). The chitosan density decreased with chitosan in solution at low concentrations until the density became relatively constant at approximately 0.4–0.6 g/L and above ($p > 0.05$), which was the same concentration at which the zeta-potential plateau was observed.

3.3. Adsorption isotherms

The adsorption of chitosan onto PLGA NPs did not comply with the Langmuir model in the wide range of chitosan concentration tested (Fig. 4A). However, the Langmuir monolayer model fits well at low initial chitosan concentrations, i.e. from 0 to 0.48 g/L. The adsorption of chitosan fits poorly with the BET model (Fig. 4B). Similarly, the BET model fits well at low initial chitosan concentrations, i.e. from 0 to 0.48 g/L. With the exceptions noted, the multi-player adsorption models including the Freundlich (Fig. 4C), Halsey (Fig. 4D), Henderson (Fig. 4E), and Smith (Fig. 4F) isotherms all fit with good agreement ($r^2 \geqslant 0.9$), and the corresponding adsorption parameters were calculated (Table 1).

4. Discussion

PLGA particulate drug delivery systems have been widely used for biomacromolecules such as peptides, proteins or nucleic acids [32,33]. A frequently used approach to load the drug into PLGA particles is by encapsulation based on single or double emulsion methods [34]. Sustained release, localized release, and *in vivo* stabilization can be achieved using PLGA particles. However, during preparation, organic solvents and shear stress can denature or deactivate the biopolymers incorporated [35,36]. PLGA particles also generate an acidic internal environment after gradual hydrolysis into lactic acid and glycolic acid, which is detrimental to biopolymer stability [37]. The encapsulation efficiency of biopolymers in the particles is essentially low and results in the consumption of a large quantity of biopolymers in the preparation. Hence, surface coating of PLGA particles was proposed in this study to avoid direct involvement of biopolymers in the harsh conditions for the preparation of PLGA particles. Biopolymers can be reconstituted with the functionalized PLGA NPs when necessary.

Chitosan was selected to coat PLGA NPs in this study because of the cationic charge, biodegradability and mucoadhesive properties [38]. In addition, chitosan-coated particles have been proposed for biomacromolecule delivery [39]. However, like other cationic polymers, the strong positive charge of chitosan contributes to the toxicity of the polymer. The amount of chitosan can be substantially decreased by making chitosan-coated PLGA NPs, because only a lower amount of chitosan was expected to coat on the surface of a particle compared to free chitosan. This is particularly true due to the large surface-to-volume ratio of the particles that were produced.

The particle size polydispersity was primarily due to the high shear ultrasonication process, during which heterogeneous energy was spread from a microtip probe in the center, but this polydispersity was similar in all the samples. The hydrodynamic diameter of chitosan-coated PLGA NPs increased gradually with initial chitosan concentration. The increased particle size could be attributed to the increased viscosity of chitosan, which lowered the shear stress on PLGA organic phase during ultrasonication and generated larger emulsion droplets [18]. Another explanation for increased particle size was that increased particle diameter was due to the increased amount of adsorbed chitosan on the surface of PLGA NPs. Not excluding the first possibility, this study showed that the latter was a viable explanation for increased particle size. This will be further supported in the continued discussion.

The zeta-potential of uncoated PLGA NPs was negative as expected because of the carboxyl end groups on PLGA. The positive zeta-potential of chitosan-coated PLGA NPs confirmed the presence of chitosan on PLGA NPs. The gradual increase of zeta-potential at low concentrations of chitosan (less than approximately 0.6 g/L; Fig. 2) indicated a gradual increase of surface chitosan until a steady surface charge was reached at high chitosan concentrations. The plateau in zeta-potential with increased initial chitosan
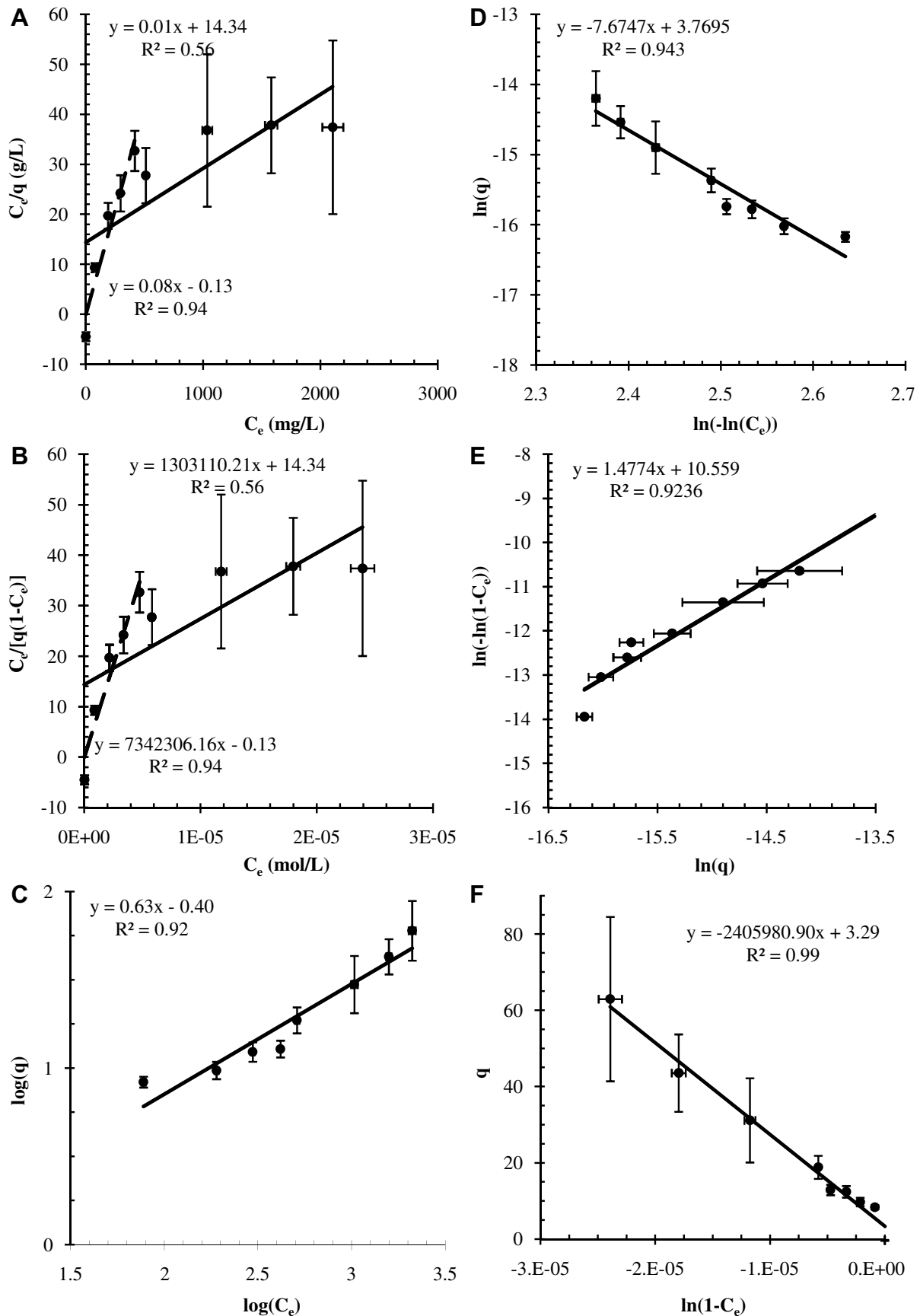
Fig. 4. Linear representation of the six isotherm models of chitosan adsorption onto PLGA NPs at pH 5.0. C_e is the residual chitosan concentrations in the suspension at equilibrium (mg/L in A; mol/L in B, C, D, E and F), and q is the amount of adsorbed chitosan per unit weight of PLGA NPs (mg/g in A, C and F; mol/g in B, D and E). The (A) Langmuir and (B) BET models were fit with two regression lines plotted for low (0–0.48 g/L) (- - -) and the entire range of concentrations (—), respectively. The (C) Freundlich, (D) Halsey, (E) Henderson, and (F) Smith models were fit whole range of concentrations. Values are presented as means ± standard deviation (n = 3).

Table 1
Parameters derived from adsorption isotherm models by linear regression

Isotherm equations	Adsorption capacity	Adsorption intensity	Regression coefficient
Langmuir[*]	$q_m = 11.9904$ mg/g	$b = -0.6490$	0.9406
BET	$q_m = 7.674 \times 10^{-7}$ mol/g	$b = 90857.4$	0.5630
Freundlich	$k = 0.4002$	$n = 1.5997$	0.9236
Halsey	$k = 1.6342$	$n = 0.1303$	0.9430
Henderson	$k = 38522.6$	$n = 1.4774$	0.9236
Smith	$w_b = 3.2855$ mg/g	$w_a = 2.406 \times 10^6$	0.9865

[*] PLGA nanoparticles made at 0–0.48 g/L chitosan initial concentration.

could be indicative of saturated adsorption of chitosan on PLGA NPs. However, the amount of adsorbed chitosan on PLGA NPs increased with the initial chitosan concentration and the saturation of adsorption was observed in the concentration tested (Fig. 3A). From this, we observed that the continued adsorption of chitosan on PLGA NPs did not affect the apparent zeta-potential at high concentrations (greater than approximately 0.4–0.6 g/L). Therefore, the layer structure of the adsorbed chitosan was further examined to understand the adsorption. As a possible model, multiple layers of chitosan only allow a small amount of chitosan to influence the zeta-potential. Layers beyond the first few do not increase the zeta-potential because the apparent surface charge per unit area (amine groups) is constant. This is supported by the calculation of the density of the chitosan layer (Fig. 3B) with increasing initial chitosan. A plateau in density is calculated to coincide with the zeta-potential plateau.

To further understand this, models of the possible chitosan chain configurations are helpful. The conformation of linear flexible polymer adsorbed onto a solid consists of adsorbed segments ("trains"), free "loops" extended away from the surface and two free dangling "tails" (Fig. 5A) [40]. Chitosan molecules are more tightly bound on the surface at low concentrations of chitosan, hence more "trains" are expected. These trains should have a high surface density due to tight electrostatic interactions with the surface. With increase in chitosan concentration, the hydrodynamic particle size increased due to significant loop and train formation, which lead to a decrease of chitosan density. At high concentrations (greater than about 0.4–0.6 g/L), as loose layers of chitosan formed on the initial tight chitosan chains, a relatively constant density of adsorbed layer was formed. When a number of layers form, the cationic chitosan molecules tend to repel each other, resulting in the formation of loose layers. Both multi-layer formation and heterotypic interactions with the surface are supported by the applied models.

Adsorption isotherms were theoretically or empirically derived from the study of the relationship between the quantity of adsor-
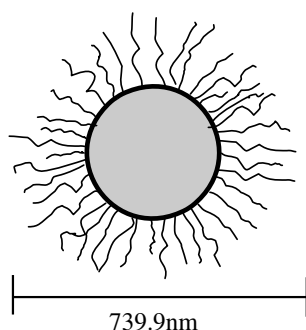

Fig. 5. Schematic representation of the brush-type conformation of adsorbed chitosan chains on PLGA NP. The theoretical diameter of a PLGA particle with coating would be 739.9 nm for the brush-type configuration if a single layer were introduced.

bate per unit of adsorbent (q) and the equilibrium adsorbate concentration (C_e). The derivation of adsorption isotherms is based on the various assumptions of the conditions of adsorption, including the properties of components and interaction between adsorbate and adsorbent. A good model fitting of the experimental data could suggest the mechanism of the adsorption from that model fits the assumptions of that particular model. The Langmuir model was developed originally for systems with a monolayer adsorption on the surface of an adsorbent [22]. This model was derived on the assumptions that all the adsorption sites are equivalent, and the adsorption is independent of surface coverage, and it occurs without lateral interaction of adsorbate molecules [41]. The Langmuir model (Fig. 4A) was valid at low concentrations (0–0.48 g/L) prior to the adsorbed layer structure change, which is typical of the Langmuir model fitting for multi-layer formation. The monolayer adsorption capacity (q_m) was found to be 11.9 mg/g PLGA NPs, which corresponded to the initial concentration of chitosan at 0.48 g/L. However, the Langmuir monolayer model could not explain adsorption at high concentrations of chitosan.

The BET (Brunauer–Emmett–Teller) model [23] did not fit the data in the whole range of concentrations (Fig. 4B). The adsorption data at low concentration (0–0.48 g/L) of chitosan fit the BET model, which is similar to the Langmuir model. The BET model was an extension of the Langmuir monolayer model to multilayer adsorption. According to the BET model, the monolayer is formed by the same mechanisms as the Langmuir type adsorption, the subsequent layers are condensation of the adsorbate molecules, and the layers beyond the first are assumed to have equal energies of adsorption, which is characteristic for a uniform surface [42]. In addition, the BET model considers only short-range interactions between adsorbate and adsorbent [43]. The adsorption phenomena presented here did not fit the model because the idealized nature of the BET model, significant adsorbate–adsorbate interactions and the non-uniform surface interactions are not expected.

The adsorption data of chitosan fit quite well with the Freundlich model [24]. The Freundlich model is perhaps the most widely used nonlinear adsorption model. Although it is empirical in its origins, the Freundlich model is thermodynamically rigorous for special cases of adsorption on heterogeneous surfaces. The Freundlich model is suitable for both a homogenous surface and a highly heterogeneous surface with a multilayer adsorption. The calculated value of n (adsorption intensity) is 1.5997, which is above 1, indicating that a beneficial adsorption of chitosan occurred on the surface of PLGA NPs [44]. Low $1/n$ values (less than unity) are indicative of greater heterogeneity in energy distribution and favorable adsorption at low concentrations [45].

The Halsey, Henderson and Smith isotherm models describe the exponential or logarithmic nature of the relationships between q and C_e, which correspond to multilayer adsorption of an adsorbate [31,46]. Each of these models are consistent with an adsorption on an energetically heterogeneous surface [46,47]. The Halsey model describes multilayer condensation at relatively large distances from a non-uniform surface. According to Halsey model [25], the typical multilayer isotherm is composed of three regions: noncooperative adsorption on a strongly heterogeneous surface; cooperative adsorption on a still heterogeneous surface; and cooperative multilayer adsorption induced by small van der Waals perturbations at some distance from the surface [48]. The Henderson model is a semi-empirical model derived on thermodynamic procedures. The large value of the constants for the Henderson model indicated a possible microporous or energetically heterogeneous structure for chitosan adsorption [49]. In the Smith model [27], the adsorbed amount on the surface is subdivided into a bound and a normally condensed fraction. The bound fraction of adsorbate is on the inner or outer surface of the solid
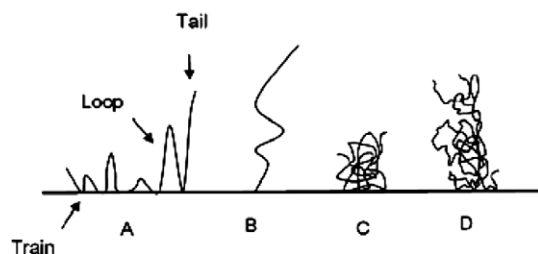
Fig. 6. Schematic representation of conformations of adsorbed chitosan chains (A) chain with trains, loops and tails, (B) chain anchored on the surface with one end, (C) adsorbed coil or aggregate, (D) interacting chains.

adsorbent by forces in excess of the normal forces for condensation. The normally condensed fraction may also have more than one condensed layer of adsorbate. The data fit quite well with the Smith model, suggesting the distinction between two classes of adsorbed chitosan molecules on PLGA NPs.

The adsorption of chitosan on PLGA NPs follows a multilayer adsorption behavior regardless of which model is considered, suggesting that the adsorption of chitosan occurred on an energetically heterogeneous surface. The morphological heterogeneity of washed particles has been demonstrated by the rough surface, and non-uniform shape observed from SEM images (Fig. 4). Chemical heterogeneity could also contribute to the adsorption, i.e. the distribution of carboxyl end groups and intermediate segments of PLGA molecules on the surface of the particles.

It is true that the Langmuir model is based on an ideal localized monolayer on uniform surface. And Langmuir warned in his early paper that the equations "which apply to adsorption by plane surfaces, could not apply to adsorption by charcoal", a porous adsorbent [22]. However, the reality is that the Langmuir equation is still used to analyze the adsorption isotherms of charcoal and it works. In this sense, the Langmuir model may be regarded as a useful empirical tool. In addition, monolayer adsorption could occur on the micropore walls at low pressure or concentration before the onset of micropore filling [50]. As demonstrated in our study, a Langmuir-like monolayer formed at low chitosan concentration on the heterogeneous surface of PLGA NPs.

The monolayer formation could also be analyzed from the aspect of chain length of chitosan molecule and the particles size of blank PLGA NPs. The chitosan used in this study is 88 kD with 85% deacetylation. The molecular weights of glucosamine unit and the acetylglucosamine unit are 161 g/mol and 203 g/mol, respectively. The average molecular weight of monomer units is calculated to be 187.6 g/mol based on 85% deacetylation. Hence, the number of monomers in a chitosan chain molecule is approximately 469. The virtual bond length per monomer unit of chitosan is reported to be 0.51 nm, regardless of the molecular weight, degree of deacetylation and ionic strength [51]. Therefore, the chain length of chitosan is 239.2 nm assuming linear arrangement of the monomers. Therefore, the monolayer thickness cannot be more than the chain length of chitosan which is 239.2 nm. Then, the diameter of particles should not exceed the sum of the diameter of PLGA blank NPs (261.5 nm) plus two chitosan chain lengths, which would total to 739.9 nm. The conformation of the coating is termed as "brush" type when there is only one end of chitosan chain attached to the surface of PLGA particles with the other end (tail) extended freely to the bulk solution (Fig. 6). It should be noted that the "brush" configuration is energetically unlikely and thus any particle that approaches this value would be expected to have multiple layers of chitosan present.

As described before, the fully surface-covered monolayer corresponded to chitosan-PLGA NPs made in 0.48 g/L chitosan, which

had a hydrodynamic diameter of 640.2 nm, well below 739.9 nm. Therefore, the monolayer is probably not of the "brush" type, which also needs high energy for terminal surface binding with only one end of the chain. Considering that the actual layer thickness is 189.4 nm, the adsorbed chains of monolayer could be a mingled conformation of A, C and/or B (Fig. 6), each of which contains trains, loops, tails or coils on the surface of particles.

Electrostatic attraction between positively charged chitosan and negatively charged PLGA surface was likely the predominant driving force especially in the formation of the first monomolecular adsorption layer. The adsorption of chitosan continued even though a positively charged surface had been achieved, in which hydrogen bond (N–H) or van der Waal's force could be involved. At high concentration, it is possible that the subsequent layers of chitosan could be adsorbed on the first layer and had no direct contact with the surface. With more layers added, chitosan chains would repel to each other due to the same charge but be attracted and interact through hydrophobic interactions, van der Waal's forces and hydrogen bonds. The adsorbed chitosan may be in the A, C or D conformations (Fig. 6), in particular the D configuration with one chain is intertwined with another chain. Basically, the small size and the high surface energy of PLGA NPs played an important role for multilayer adsorption of chitosan.

5. Conclusion

Cationic nanoparticles were prepared by coating chitosan on the surface of PLGA NPs, and the adsorption mechanism was investigated. The diameter of PLGA NPs increased with the initial chitosan concentration primarily due to the increased amount of adsorbed chitosan on the surface. The zeta-potential of chitosan-PLGA particles increased with the initial chitosan concentration until a plateau was reached at approximately 0.4–0.6 g/L while the mass of adsorbed chitosan on PLGA NPs increased with chitosan concentration in the range of 0–2.4 g/L. The continued adsorption of chitosan on the surface did not affect the maximum zeta-potential obtained. Six adsorption isotherms (Langmuir, BET, Freundlich, Halsey, Henderson, and Smith) models were used to describe the adsorption of chitosan onto PLGA NPs. The adsorption of chitosan on PLGA NPs complied with a multilayer adsorption behavior on a heterogeneous surface. A better understanding of the interaction between polyelectrolyte and polyesters materials will be beneficial to further design the efficient gene delivery systems.

References

[1] I. Bala, S. Hariharan, M.N. Kumar, Plga nanoparticles in drug delivery: the state of the art, Crit. Rev. Ther. Drug Carrier Syst. 21 (5) (2004) 387–422.
[2] H. Okada, H. Toguchi, Biodegradable microspheres in drug delivery, Crit. Rev. Ther. Drug Carrier Syst. 12 (1) (1995) 1–99.
[3] M.E. Keegan, J.A. Whittum-Hudson, W.M. Saltzman, Biomimetic design in microparticulate vaccines, Biomaterials 24 (24) (2003) 4435–4443.
[4] M.E. Keegan, J.L. Falcone, T.C. Leung, W.M. Saltzman, Biodegradable microspheres with enhanced capacity for covalently bound surface ligands, Macromolecules 37 (26) (2004) 9779–9784.
[5] M. Singh, J. Kazzaz, M. Ugozzoli, J. Chesko, D.T. O'Hagan, Charged polylactide co-glycolide microparticles as antigen delivery systems, Expert Opin. Biol. Ther. 4 (4) (2004) 483–491.

[6] A. Ulusoy, M.A. Onur, Measurement of in vitro phagocytic activity using functional groups carrying monodisperse poly(glycidyl methacrylate) microspheres in rat blood, J. Biomater. Sci. Polym. Ed. 14 (11) (2003) 1299–1310.

[7] B. Mandal, M. Kempf, H.P. Merkle, E. Walter, Immobilisation of gm-csf onto particulate vaccine carrier systems, Int. J. Pharm. 269 (1) (2004) 259–265.

[8] Z. Cui, R.J. Mumper, Genetic immunization using nanoparticles engineered from microemulsion precursors, Pharm. Res. 19 (7) (2002) 939–946.

[9] M. Singh, J. Kazzaz, M. Ugozzoli, P. Malyala, J. Chesko, D.T. O'Hagan, Polylactide-co-glycolide microparticles with surface adsorbed antigens as vaccine delivery systems, Curr. Drug Deliv. 3 (1) (2006) 115–120.

[10] M. Bivas-Benita, S. Romeijn, H.E. Junginger, G. Borchard, Plga-pei nanoparticles for gene delivery to pulmonary epithelium, Eur. J. Pharm. Biopharm. 58 (1) (2004) 1–6.

[11] Y.H. Kim, J.H. Park, M. Lee, Y.H. Kim, T.G. Park, S.W. Kim, Polyethylenimine with acid-labile linkages as a biodegradable gene carrier, J. Control. Release 103 (1) (2005) 209–219.

[12] C.G. Oster, N. Kim, L. Grode, L. Barbu-Tudoran, A.K. Schaper, S.H.E. Kaufmann, T. Kissel, Cationic microparticles consisting of poly(lactide-co-glycolide) and polyethylenimine as carriers systems for parental DNA vaccination, J. Control. Release 104 (2) (2005) 359–377.

[13] M. Muller, J. Voros, G. Csucs, E. Walter, G. Danuser, H.P. Merkle, N.D. Spencer, M. Textor, Surface modification of PLGA microspheres, J. Biomed. Mater. Res. A 66 (1) (2003) 55–61.

[14] M. Kumar, U. Bakowsky, C.M. Lehr, Preparation and characterization of cationic PLGA nanospheres as DNA carriers, Biomaterials 25 (10) (2004) 1771–1777.

[15] M.N. Kumar, S.S. Mohapatra, X. Kong, P.K. Jena, U. Bakowsky, C.M. Lehr, Cationic poly(lactide-co-glycolide) nanoparticles as efficient in vivo gene transfection agents, J. Nanosci. Nanotechnol. 4 (8) (2004) 990–994.

[16] M.J. Tsung, D.J. Burgess, Preparation and characterization of gelatin surface modified plga microspheres, AAPS PharmSci. 3 (2) (2001) E11.

[17] S. Munier, I. Messai, T. Delair, B. Verrier, Y. Ataman-Onal, Cationic pla nanoparticles for DNA delivery: comparison of three surface polycations for DNA binding, protection and transfection properties, Colloids Surf. B Biointerfaces 43 (3–4) (2005) 163–173.

[18] S. Fischer, C. Foerg, S. Ellenberger, H.P. Merkle, B. Gander, One-step preparation of polyelectrolyte-coated plga microparticles and their functionalization with model ligands, J. Control. Release 111 (1–2) (2006) 135–144.

[19] I. Messai, T. Delair, Adsorption of chitosan onto poly(D,L-lactic acid) particles: a physico-chemical investigation, Macromol. Chem. Phys. 206 (16) (2005) 1665–1674.

[20] S. Udenfriend, S. Stein, P. Bohlen, W. Dairman, W. Leimgruber, M. Weigele, Fluorescamine: a reagent for assay of amino acids, peptides, proteins, and primary amines in the picomole range, Science 178 (63) (1972) 871–872.

[21] Y.N. Lin, T.W. Smith, P. Alexandridis, Adsorption of a polymeric siloxane surfactant on carbon black particles dispersed in mixtures of water with polar organic solvents, J. Colloid Interface Sci. 255 (1) (2002) 1–9.

[22] I. Langmuir, The constitution and fundamental properties of solids and liquids. Part1. Solids, J. Am. Chem. Soc. 38 (11) (1916) 2221–2295.

[23] S.E. Brunauer, P.H. Teller, Edward Adsorption of gases in multimolecular layers, J. Am. Chem. Soc. 60 (1938) 309–319.

[24] H. Freundlich, Colloid and Capillary Chemistry, Methuen & Co., London, 1926.

[25] G. Halsey, Physical adsorption on non-uniform surfaces, J. Chem. Phys. 16 (10) (1948) 931–937.

[26] S.M. Henderson, A basic concept of equilibrium moisture content, Agric. Eng. 33 (2) (1952) 39–42.

[27] S.E. Smith, The sorption of water vapor by high polymers, J. Am. Chem. Soc. 69 (1947) 646–651.

[28] A.E.R. Baldev Raj, K.R. Kumar Siddarramaiah, Moisture–sorption characteristics of starch/low-density polyethylene films, J. Appl. Polym. Sci. 84 (6) (2002) 1193–1202.

[29] C.A. Basar, Applicability of the various adsorption models of three dyes adsorption onto activated carbon prepared waste apricot, J. Hazard. Mater. 135 (1–3) (2006) 232–241.

[30] M. Erbas, M.F. Ertugay, M. Certel, Moisture adsorption behaviour of semolina and farina, J. Food Eng. 69 (2) (2005) 191–198.

[31] S. Karaca, A. Gurses, R. Bayrak, Investigation of applicability of the various adsorption models of methylene blue adsorption onto lignite/water interface, Energ. Convers. Manage. 46 (1) (2005) 33–46.

[32] J. Panyam, V. Labhasetwar, Biodegradable nanoparticles for drug and gene delivery to cells and tissue, Adv. Drug Deliv. Rev. 55 (3) (2003) 329–347.

[33] H. Takeuchi, H. Yamamoto, Y. Kawashima, Mucoadhesive nanoparticulate systems for peptide drug delivery, Adv. Drug Deliv. Rev. 47 (1) (2001) 39–54.

[34] R. Jalil, J.R. Nixon, Biodegradable poly(lactic acid) and poly (lactide-co-glycolide) microcapsules: Problems associated with preparative techniques and release properties, J. Microencapsul. 7 (3) (1990) 297–325.

[35] M. van de Weert, W.E. Hennink, W. Jiskoot, Protein instability in poly(lactic-co-glycolic acid) microparticles, Pharm. Res. 17 (10) (2000) 1159–1167.

[36] E. Walter, K. Moelling, J. Pavlovic, H.P. Merkle, Microencapsulation of DNA using poly(D,L-lactide-co-glycolide): stability issues and release characteristics, J. Control. Release 61 (3) (1999) 361–734.

[37] K. Fu, D.W. Pack, A.M. Klibanov, R. Langer, Visual evidence of acidic environment within degrading poly(lactic-co-glycolic acid) (PLGA) microspheres, Pharm. Res. 17 (1) (2000) 100–106.

[38] M.N. Kumar, R.A. Muzzarelli, C. Muzzarelli, H. Sashiwa, A.J. Domb, Chitosan chemistry and pharmaceutical perspectives, Chem. Rev. 104 (12) (2004) 6017–6084.

[39] M. Prabaharan, J.F. Mano, Chitosan-based particles as controlled drug delivery systems, Drug Deliv. 12 (1) (2005) 41–57.

[40] R.R. Tatsuo Sato, Stabilization of Colloidal Dispersions by Polymer Adsorption, Marcel Dekker Inc., New York, 1990.

[41] P.W. Atkins, Physical Chemistry, Oxford University Press, 1982.

[42] W.J. Weber, Adsorption theory concepts and models, in: F.L. Slejko (Ed.), Adsorption Technology: A Step-by-step Approach to Process Evaluation and Application, Marcel Dekker, Inc., New York, 1985, pp. 1–35.

[43] G.B. Kasting, N.D. Barai, Equilibrium water sorption in human stratum corneum, J. Pharm. Sci. 92 (8) (2003) 1624–1631.

[44] S. Ghorai, K.K. Pant, Investigations on the column performance of fluoride adsorption by activated alumina in a fixed-bed, Chem. Eng. J. 98 (1–2) (2004) 165–173.

[45] S. Mukherji, Adsorption of organic compounds, in: J.H. Lehr, N.J. Hoboken (Eds.), Water Encyclopedia, vol. 4, John Wiley & Sons, 2005, pp. 384–388.

[46] M.J. Rosen, Surfactants and Interfacial Phenomena, Wiley, New York, 1978.

[47] A.W. Adamson, Physical Chemistry of Surfaces, Wiley, New York, 1976.

[48] J. Chirife, H.A. Iglesias, Equations for fitting water sorption isotherms of foods. Part 1: A review, J. Food Technol. 13 (1978) 159–174.

[49] K. Boki, S. Ohno, Equilibrium isotherm equations to represent moisture sorption on starch, J. Food Sci. 56 (4) (1991) 1106–1107.

[50] K.S.W. Sing, Historical perspectives of physical adsorption, in: J. Fraissard (Ed.), Physical Adsorption: Experiment Theory and Applications, vol. 491, Kluwer Academic Publishers, Boston, 1997, pp. 3–8.

[51] J.Y. Cho, M.C. Heuzey, A. Begin, P.J. Carreau, Viscoelastic properties of chitosan solutions: effect of concentration and ionic strength, J. Food Eng. 74 (4) (2006) 500–515.